Measurement of the W and Z cross section at $\sqrt{s}$ = 13.6 TeV

Mihaela Marinescu

Birmingham HEP Seminar

8 May 2024

W and Z physics @ LHC

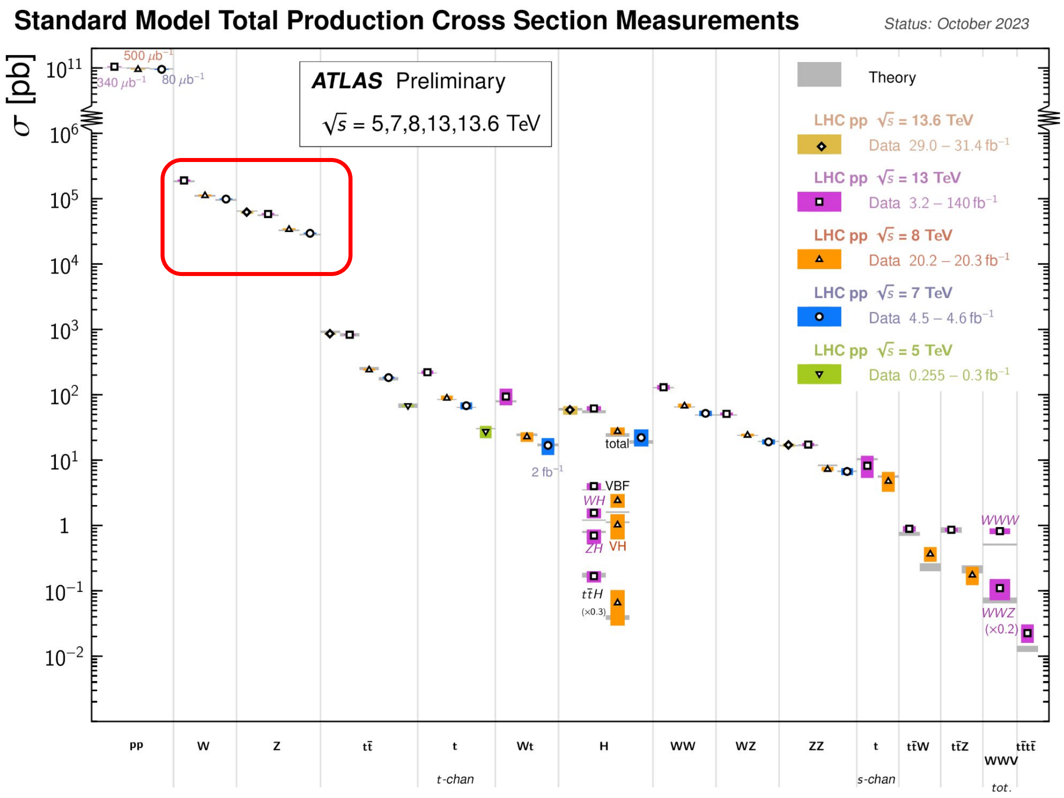

[SM public plots](#)

- Production of W/Z bosons at the LHC is of fundamental theoretical and experimental importance
  - Excellent experimental precision due to **large cross sections** and **clean experimental signature** from leptonic decays
  - Comparing measurements to theoretical predictions are an important test of perturbative QCD

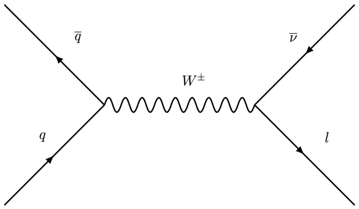

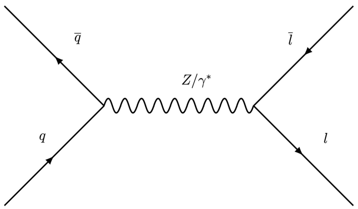

Why measure the W and Z production?

W and Z physics @ LHC

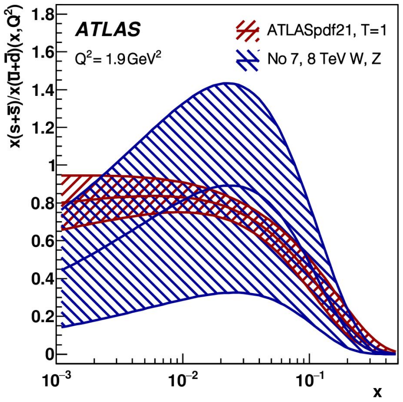

Why measure the W and Z production?

- Increase our understanding of parton distribution functions (PDFs)

W and Z physics @ LHC

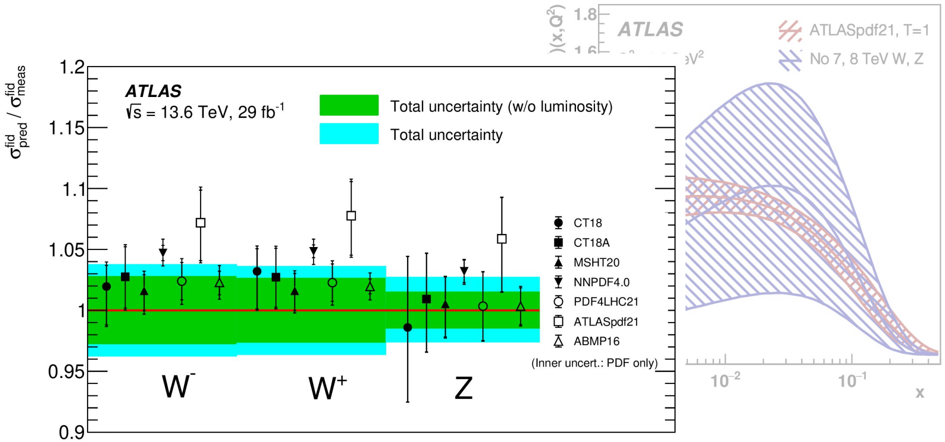

Why measure the W and Z production?

- Increase our understanding of parton distribution functions (PDFs)
- Test state-of-the-art theoretical predictions

W and Z physics @ LHC

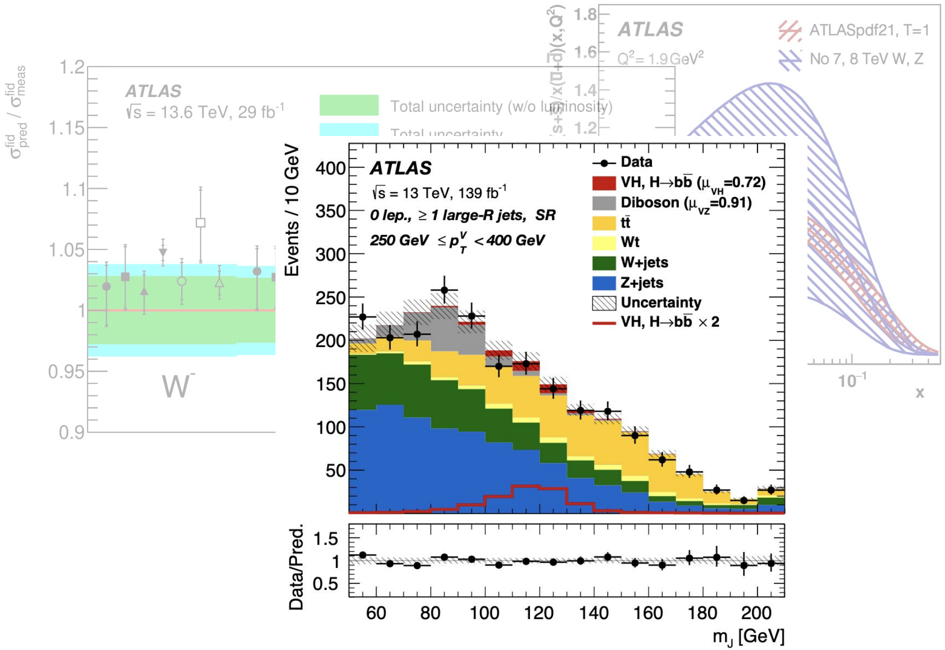

Why measure the W and Z production?

- Increase our understanding of parton distribution functions (PDFs)
- Test state-of-the-art theoretical predictions
- Improve background modelling for other measurements and searches (BSM, Higgs, etc.)

W and Z physics @ LHC

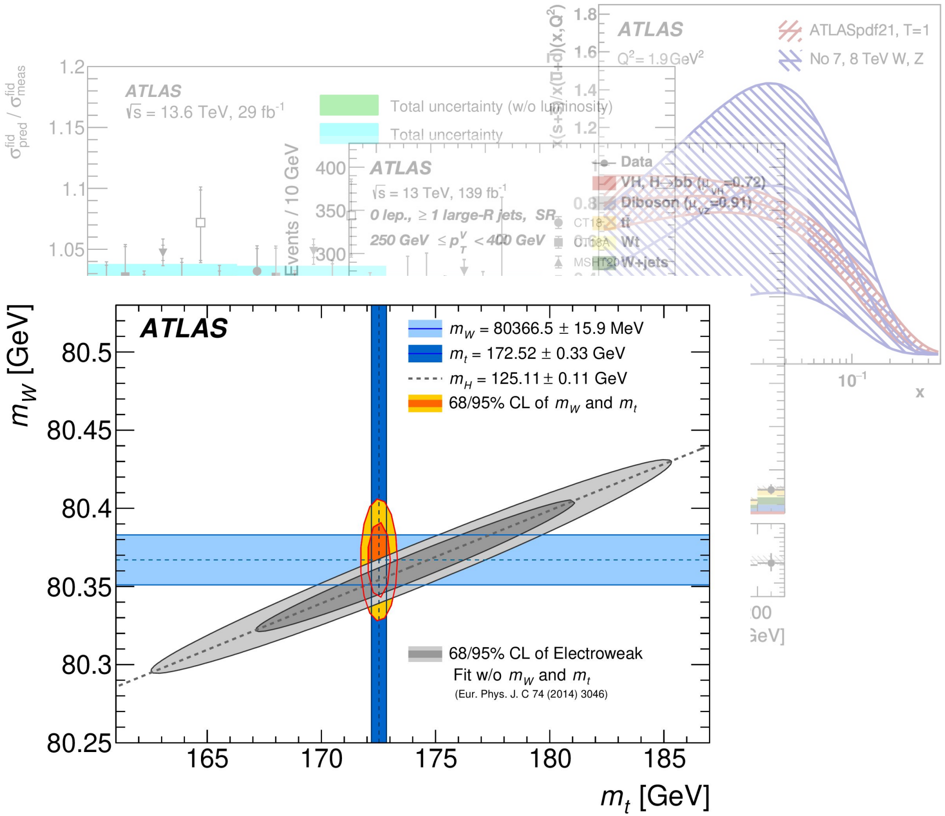

Why measure the W and Z production?

- Increase our understanding of parton distribution functions (PDFs)
- Test state-of-the-art theoretical predictions
- Improve background modelling for other measurements and searches (BSM, Higgs, etc.)
- Determination of SM parameters (m_W, $\sin^2\theta^\ell_{eff}$, …)

W and Z physics @ LHC

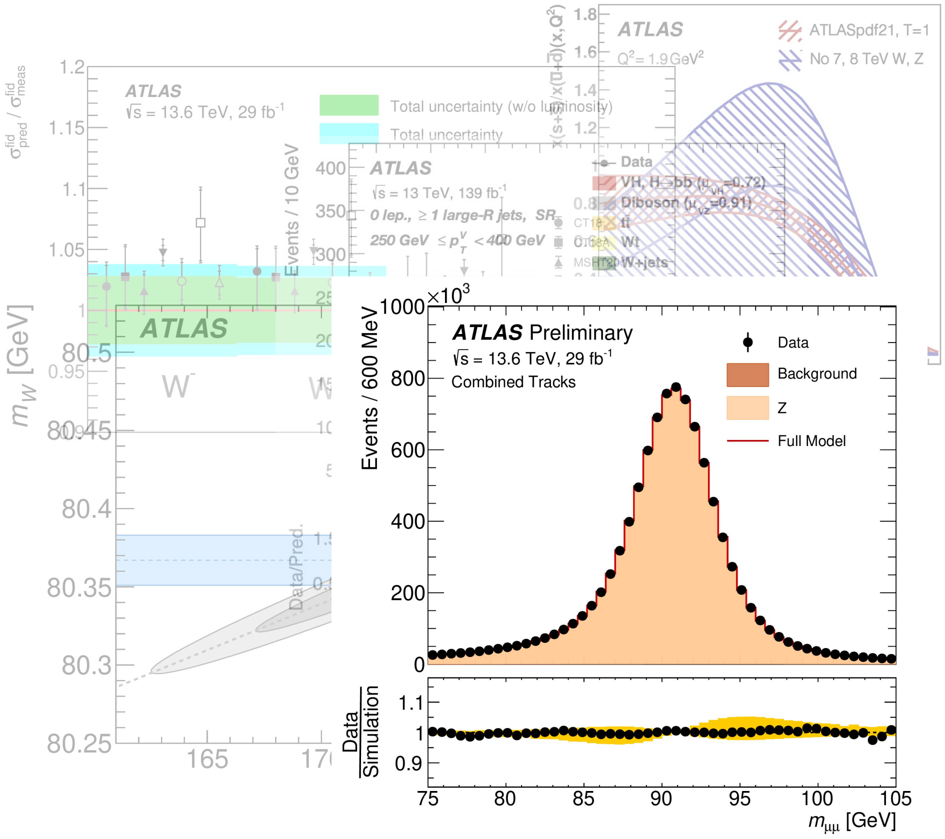

Why measure the W and Z production?

- Increase our understanding of parton distribution functions (PDFs)
- Test state-of-the-art theoretical predictions
- Improve background modelling for other measurements and searches (BSM, Higgs, etc.)
- Determination of SM parameters (m_W, $\sin^2\theta^\ell_{eff}$, …)
- Detector performance

W and Z physics @ LHC

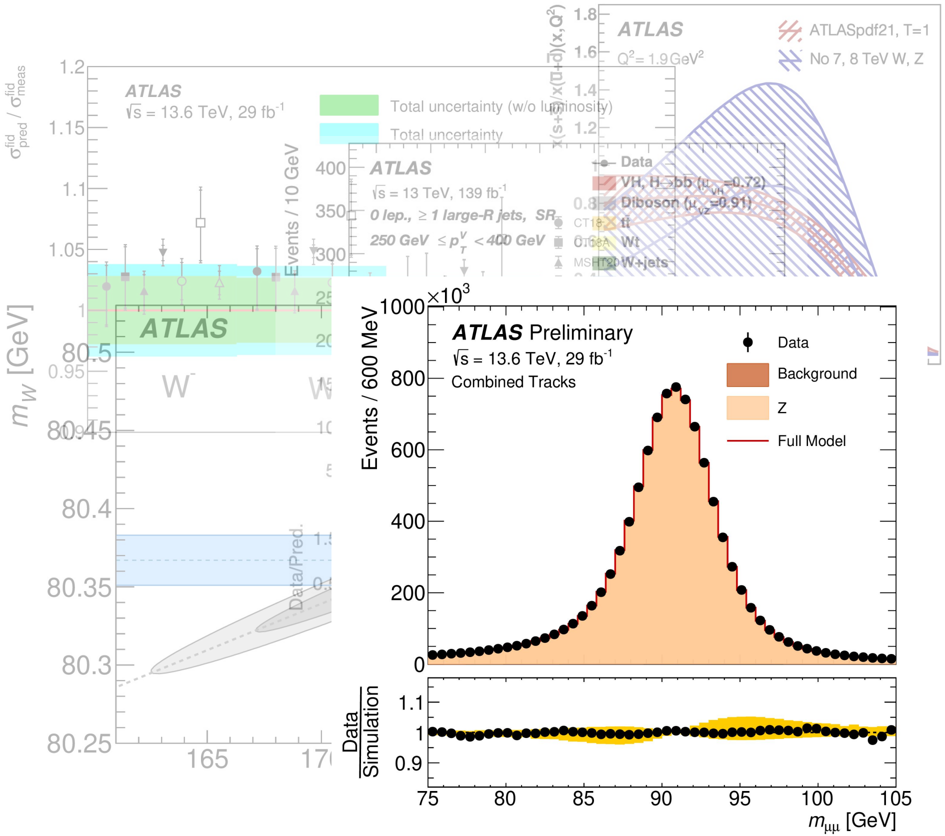

Why measure the W and Z production?

- Increase our understanding of parton distribution functions (PDFs)
- Test state-of-the-art theoretical predictions
- Improve background modelling for other measurements and searches (BSM, Higgs, etc.)
- Determination of SM parameters (m_W, $\sin^2\theta^\ell_{\mathrm{eff}}$, …)
- Detector performance

Parton distribution functions

arXiv:1709.04922

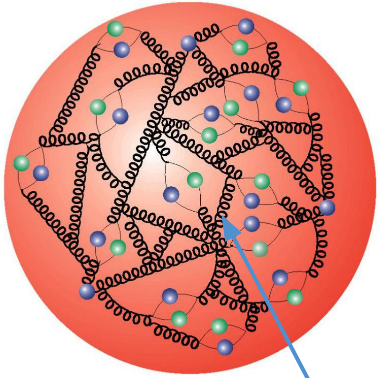

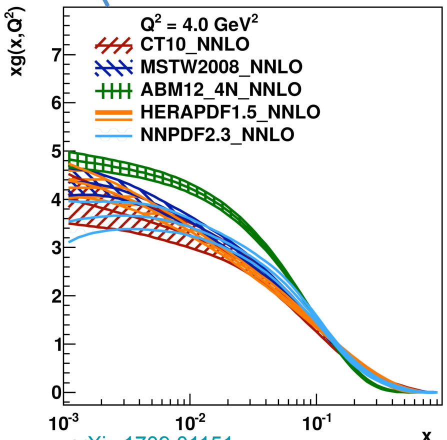

arXiv:1709.01151

- PDFs describe the probability density function of the longitudinal momentum fraction x at energy scale Q^2 for partons in the proton
- Any physics prediction at the LHC requires knowledge of PDFs
  - Essential for calculating cross sections and event generation
  - Uncertainties on PDFs translate into uncertainties on modelling and on the final measurement
- Driven by low-scale non-perturbative QCD - cannot be computed from first principles
  - Instead determined by data through global PDF fits
- Different PDF sets provided by different collaborations
  - Differences arise from datasets used, theoretical calculation of cross sections, methodological choices for parametrisation of PDFs, uncertainty estimates, etc.

Constraining PDFs using W/Z production

arXiv:1709.04922

- Inclusive W/Z production measurements are one of the key processes used in global PDF fits
- Lowest order contributions to W and Z production proceed via:

$$u\bar{d},\ c\bar{s} \quad (u\bar{s},\ c\bar{d}) \rightarrow W^+$$
$$d\bar{u},\ s\bar{c} \quad (s\bar{u},\ d\bar{c}) \rightarrow W^-$$
$$q\bar{q} \rightarrow Z/\gamma^*$$

Eur. Phys. J. C 82 (2022) 438

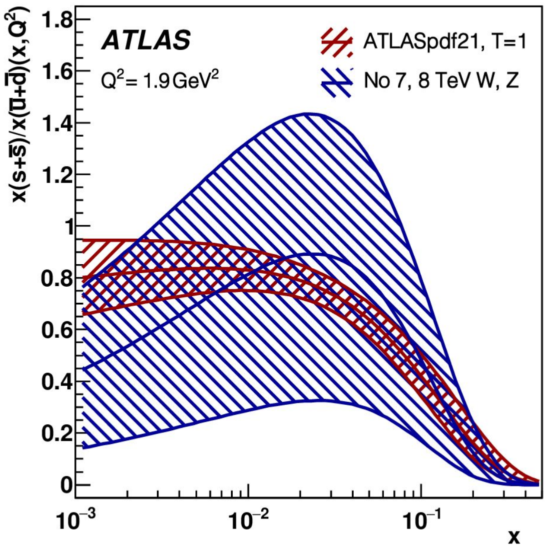

- W^+/W^- ratios sensitive to valence quark PDFs, W/Z ratios sensitive to strange quark PDFs
- Most recent global PDF fit done by ATLAS, ATLASPDF21, used large sample of ATLAS data (and ep HERA data)
  - W/Z inclusive production, ttbar, W/Z+jets, inclusive jets, direct photon production in order to sample a wide range of the x and Q^2 plane
  - W/Z data constrains strange to light sea quarks ratio at low-x
- PDF uncertainties are the leading contributions to theoretical uncertainties on measurements at the LHC
  - Measurements of Higgs couplings and EW parameters
  - Beyond-the-Standard-Model (BSM) searches

W and Z measurements for detector performance

Tag-and-Probe method

[L1Calo public plots](#)

- Use known resonance (eg. $Z \to \ell\ell$) to provide an unbiased sample of physics objects
- One lepton (tag) meets strict selection requirements, while the other lepton (probe) is used as an unbiased object
- Method used to determine the efficiency at each step of the electron/muon reconstruction stage
  - Reconstruction, identification and isolation (later slides)
  - Trigger performance

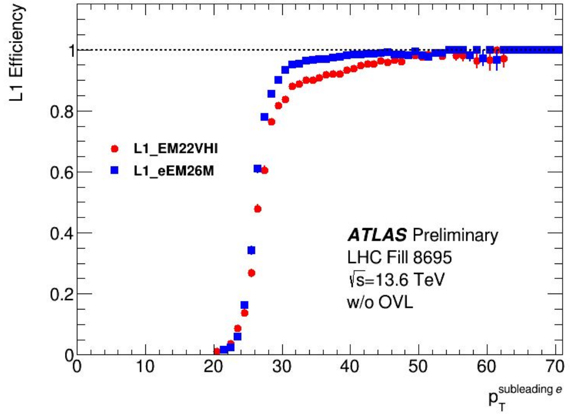

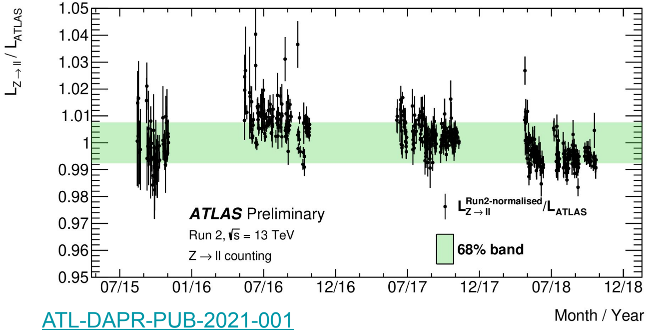

ATL-DAPR-PUB-2021-001

Luminosity determination using $Z \to \ell\ell$ events

- Counting Z bosons provides an independent check on luminosity measurement
- Can also be used to monitor luminosity, with a time granularity of about 60 s

$$\mathcal{L} = \frac{N}{\sigma}$$

The ATLAS detector in Run-3

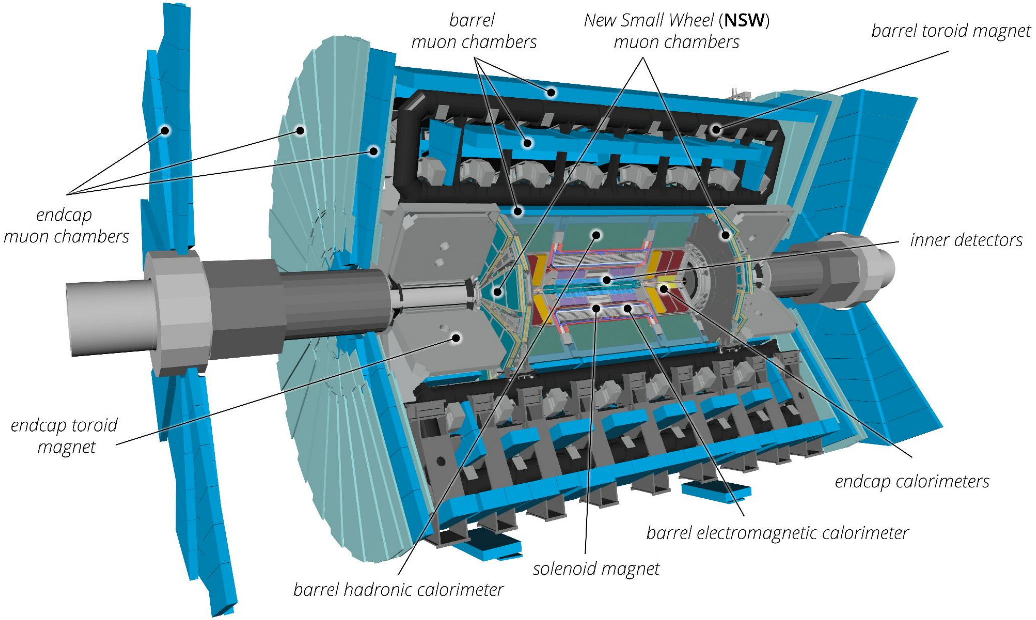

- **Inner Detector:** silicon-based pixel and semiconductor tracker, transition radiation tracker (TRT)
- **Calorimeters:** liquid argon (LAr) and Tile calorimeters
- **Muon Spectrometer:** precision tracking chambers, trigger chambers
- **Trigger:** filters interesting events using custom hardware (Level-1: 40 MHz → 100 kHz) and software-based trigger (HLT: 100 kHz → 1 kHz)

The ATLAS detector in Run-3

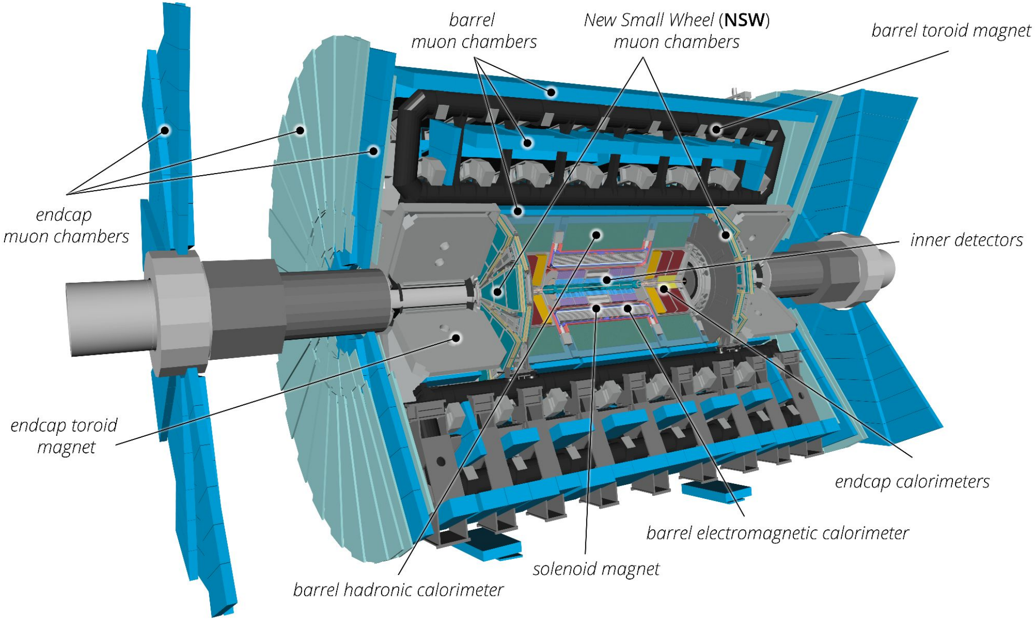

Run-3 upgrades:

- **New Small Wheel (NSW):** innermost muon station in forward region replaced with completely new detector to provide good trigger and tracking at endcap with high background rates towards HL-LHC

The ATLAS detector in Run-3

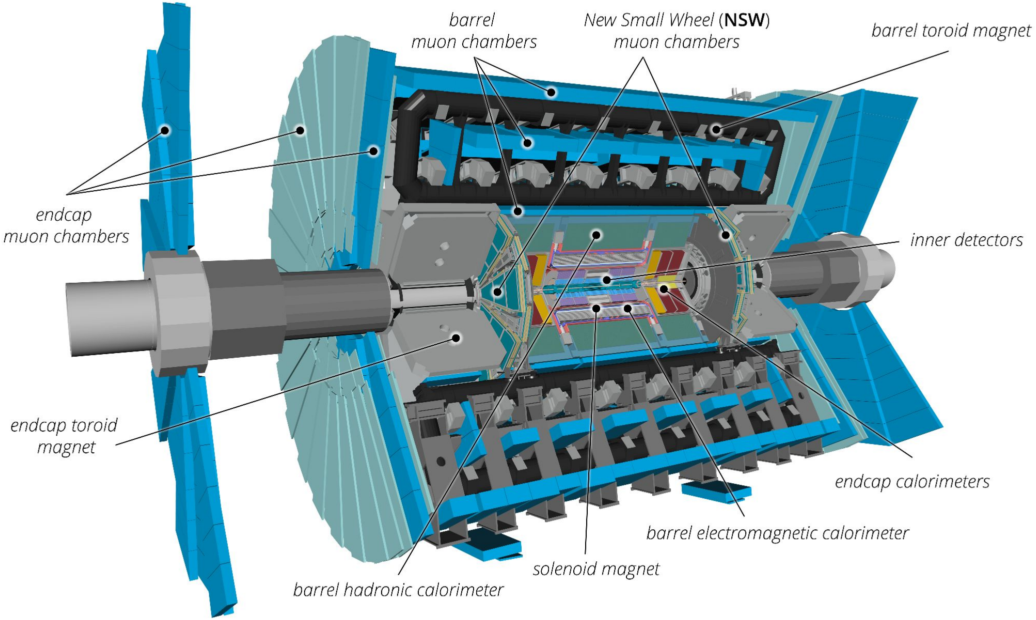

Run-3 upgrades:

- New Small Wheel (NSW)
- **LAr Calorimeter electronics:** increased readout granularity by replacing coarse trigger towers with supercells → improvement for L1 trigger at higher luminosities and pileup

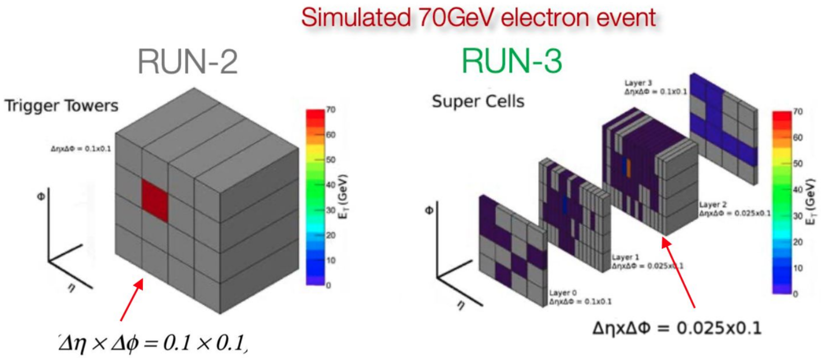

Slides by Liang Guan

The ATLAS detector in Run-3

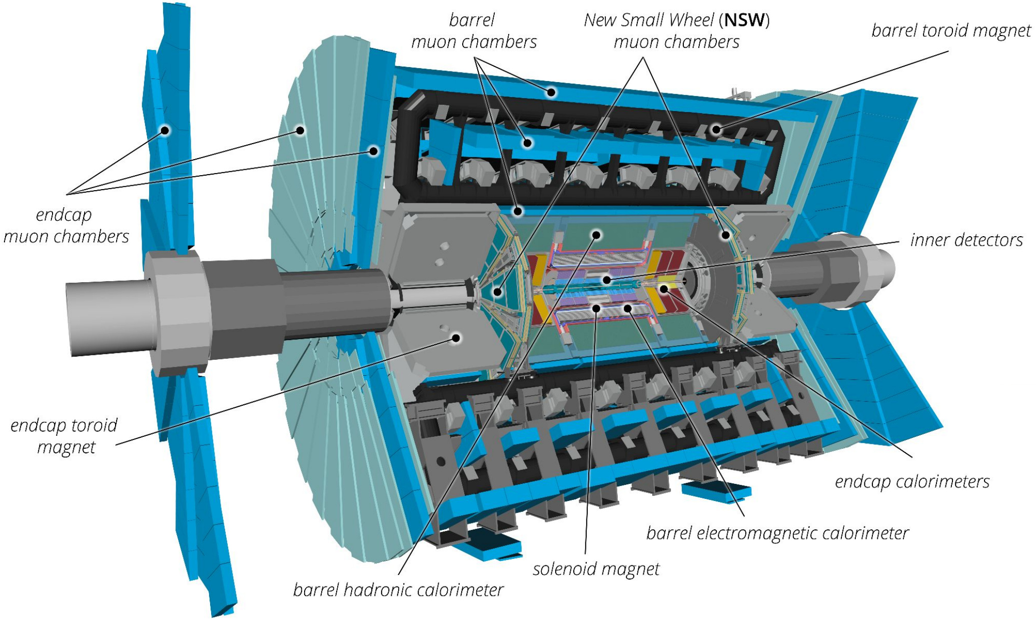

Run-3 upgrades:

- New Small Wheel (NSW)
- LAr Calorimeter electronics
- **Trigger and data acquisition (TDAQ):** new L1 hardware, new readout system

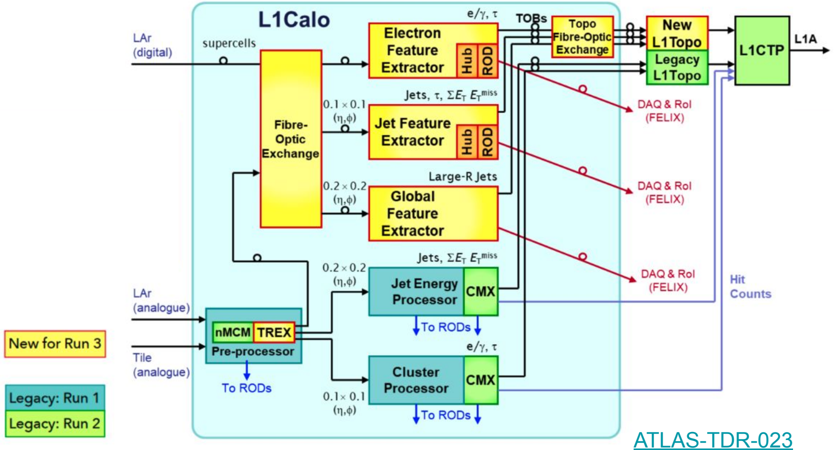

ATLAS-TDR-023

Muons

Eur. Phys. J. C 81 (2021) 578

Slides by Davide Cieri

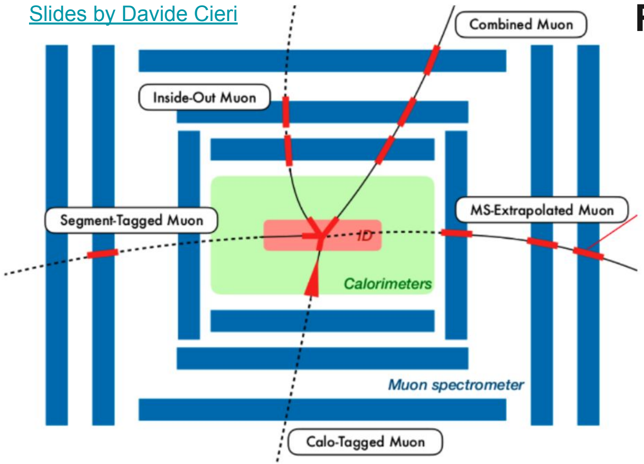

Reconstruction & Identification

- Muons are reconstructed using information from the Muon Spectrometer (MS), the Inner Detector (ID) and the Calorimeter
- **Combined muons** (95% of muons used for analysis) are identified by matching MS tracks to the ID tracks and performing a combined fit
    - Other algorithms help recover muon reconstruction efficiency at low p_T or in regions of limited detector coverage
- **ID/quality** working points are defined based on purity level and kinematics
    - Loose: high efficiency but low purity and large systematics
    - Medium: suitable efficiency and purity with low systematics

Muons

Eur. Phys. J. C 81 (2021) 578

Slides by Davide Cieri

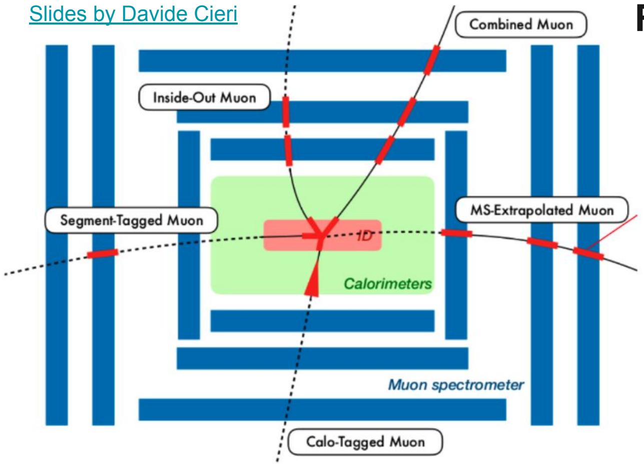

Reconstruction & Identification

- Muons are reconstructed using information from the Muon Spectrometer (MS), the Inner Detector (ID) and the Calorimeter
- **Combined muons** (95% of muons used for analysis) are identified by matching MS tracks to the ID tracks and performing a combined fit
  - Other algorithms help recover muon reconstruction efficiency at low p_T or in regions of limited detector coverage
- **ID/quality** working points are defined based on purity level and kinematics
  - Loose: high efficiency but low purity and large systematics
  - Medium: suitable efficiency and purity with low systematics

- **Muon reconstruction & ID efficiency**: measured using Tag & Probe method from Z $\rightarrow \mu\mu$ or J/$\psi \rightarrow \mu\mu$ decays
  - “Tag” muon triggers event and passes tight criteria, “probe” muon is used to test efficiency of a certain reconstruction algorithm or ID working point
  - The deviation of the simulation from the detector behavior is estimated by a scale factor (efficiencies ratio) that is used to correct the simulation

$$\varepsilon(X) = \frac{N_{\mathrm{matches}}(X)}{N_{\mathrm{probes}}}$$

$N_{\mathrm{matches}}(X)$ is the number of probes matched to a muon candidate identified with the algorithm X

Muons

[Eur. Phys. J. C 81 (2021) 578]

[Slides by Davide Cieri]

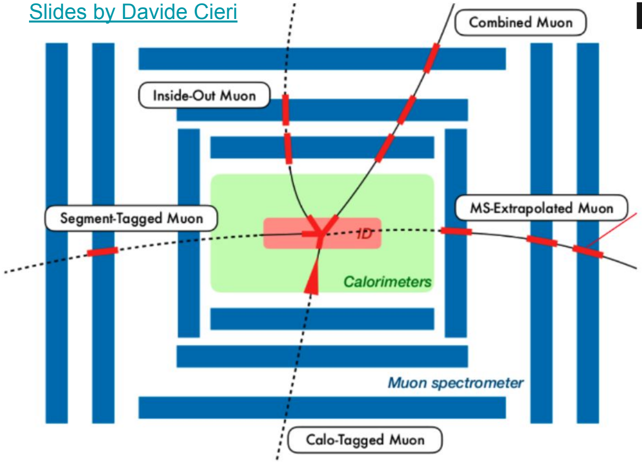

Reconstruction & Identification

- Muons are reconstructed using information from the Muon Spectrometer (MS), the Inner Detector (ID) and the Calorimeter
- **Combined muons** (95% of muons used for analysis) are identified by matching MS tracks to the ID tracks and performing a combined fit
  - Other algorithms help recover muon reconstruction efficiency at low p_T or in regions of limited detector coverage
- **ID/quality** working points are defined based on purity level and kinematics
  - Loose: high efficiency but low purity and large systematics
  - Medium: suitable efficiency and purity with low systematics

- **Muon reconstruction & ID efficiency**: measured using Tag & Probe method from $Z \rightarrow \mu\mu$ or $J/\psi \rightarrow \mu\mu$ decays
  - "Tag" muon triggers event and passes tight criteria, "probe" muon is used to test efficiency of a certain reconstruction algorithm or ID working point
  - The deviation of the simulation from the detector behavior is estimated by a scale factor (efficiencies ratio) that is used to correct the simulation

[Muon public plots]

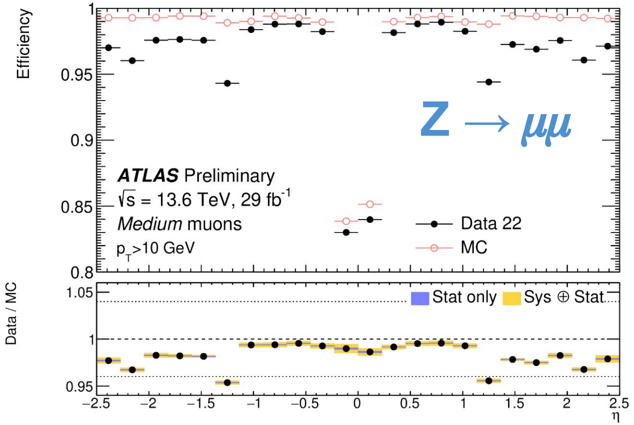

Muons

Eur. Phys. J. C 83 (2023) 686

Charge-dependent momentum scale calibration

- Charge-dependent bias on muon momentum scale introduced by imperfect knowledge of the real detector geometry
- Reconstructed Z mass from $Z \rightarrow \mu\mu$ decays is sensitive to the bias through its impact on the variance of $m_{\mu\mu}$ distribution
  - Biases used to correct muon p_T evaluated by minimising variance of $m_{\mu\mu}$ distribution in η-φ grid
  - **Correction applied to data** - simulation already assumes ideal detector alignment

Slides by Davide Cieri

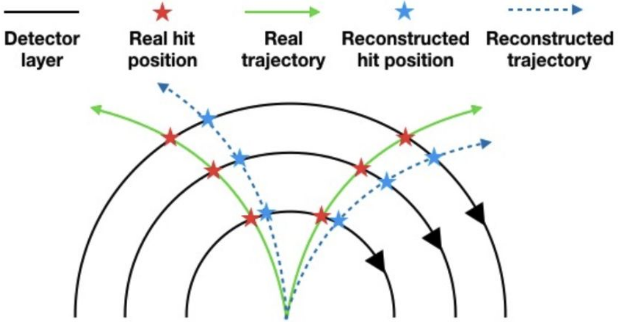

Muons

[Eur. Phys. J. C 83 (2023) 686](#)

[Muon public plots](#)

Charge-dependent momentum scale calibration

- Charge-dependent bias on muon momentum scale introduced by imperfect knowledge of the real detector geometry
- Reconstructed Z mass from $Z \to \mu\mu$ decays is sensitive to the bias through its impact on the variance of $m_{\mu\mu}$ distribution
  - Biases used to correct muon p_T evaluated by minimising variance of $m_{\mu\mu}$ distribution in η-φ grid
  - **Correction applied to data** - simulation already assumes ideal detector alignment

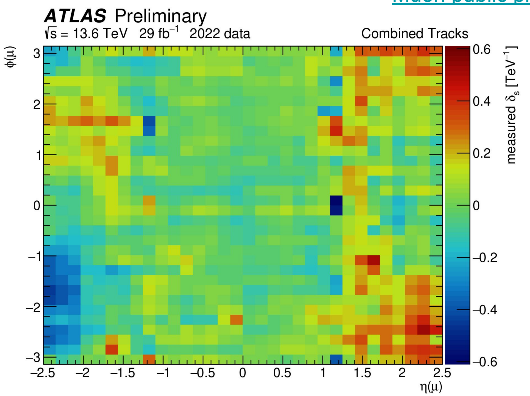

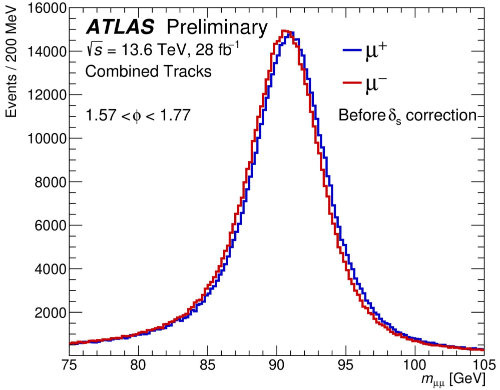

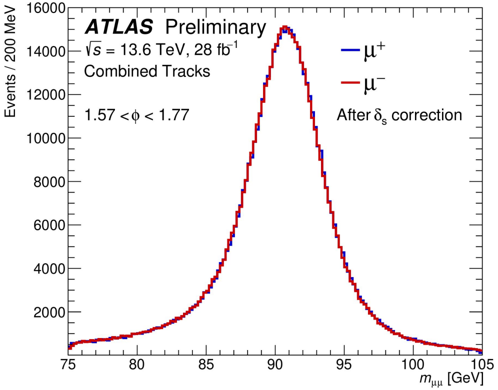

Charge-dependent bias maps correctly calibrate the muon momentum

Muons

Eur. Phys. J. C 83 (2023) 686

Muon momentum calibration

- Performed to correct mis-modelling effects in **simulation**
  - **Muon momentum scale** correction accounts for inaccuracy in description of magnetic field and energy loss in calorimeter
  - **Muon momentum resolution smearing** accounts for energy loss fluctuation in the material, multiple scattering, intrinsic detector resolution and residual misalignment
  - Corrections are extracted by fitting the $Z \rightarrow \mu\mu$ and $J/\psi \rightarrow \mu\mu$ invariant mass spectra to provide the best agreement between simulation and data

Muon public plots

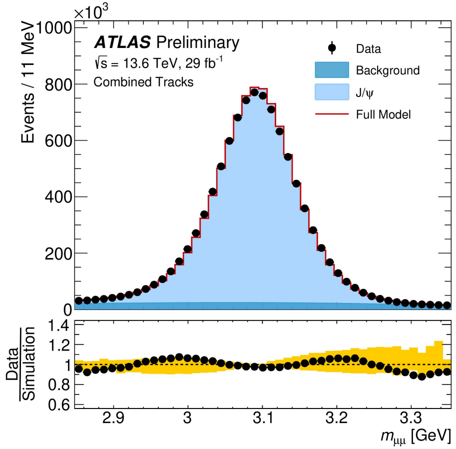

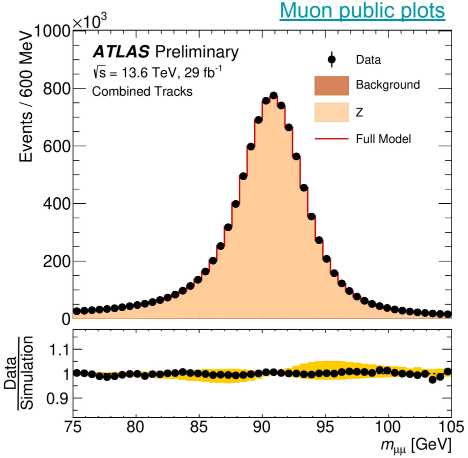

data/simulation agreement after momentum scale and smearing calibration

Electrons

[Eur. Phys. J. C 79 (2019) 639](#)
[JINST 19 (2024) P02009](#)

Reconstruction

- Electrons are reconstructed using energy deposits in the electromagnetic calorimeter and tracks from the Inner Detector (ID)
  - Dynamic, variable-sized clusters of calorimeter cells (superclusters) are used in order to recover energy from Bremsstrahlung photons or conversion electrons
- An electron candidate is identified as a supercluster matching a track reconstructed in the ID
  - If a match is found, the track is re-fitted to account for Bremsstrahlung
- **Electron reconstruction efficiency**: measured using Tag & Probe method from $Z \to ee$ decays

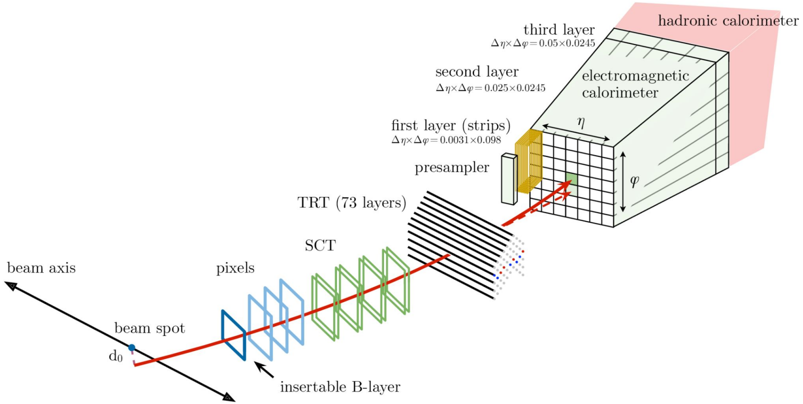

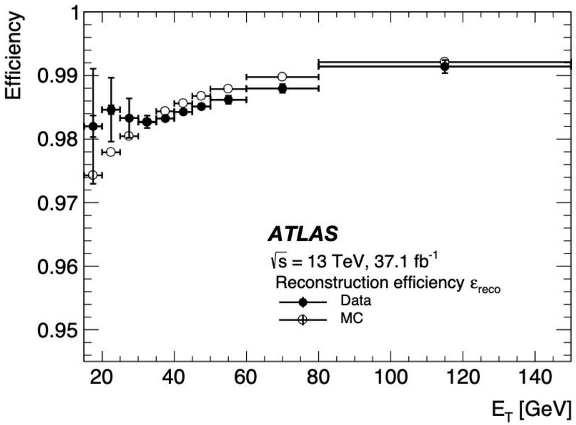

Electrons

Eur. Phys. J. C 79 (2019) 639
JINST 19 (2024) P02009

Energy calibration

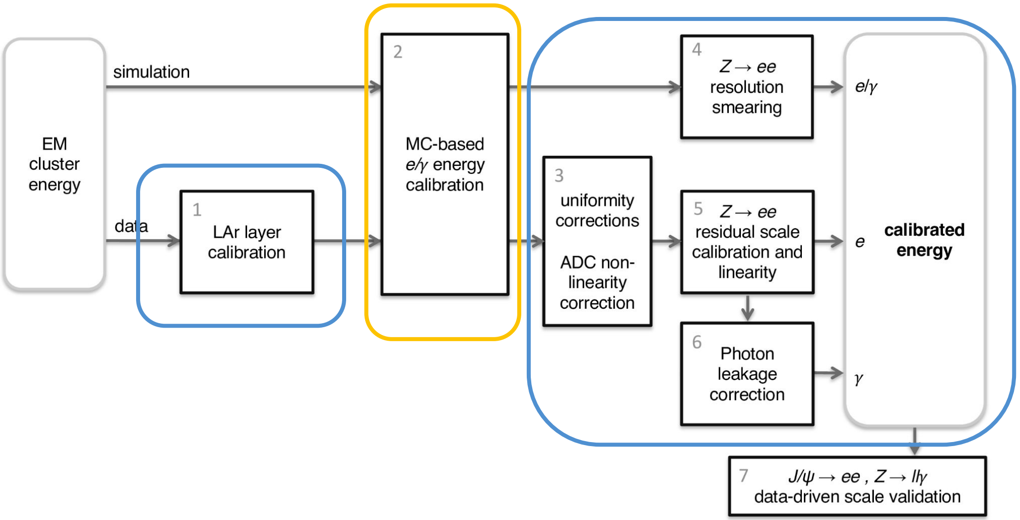

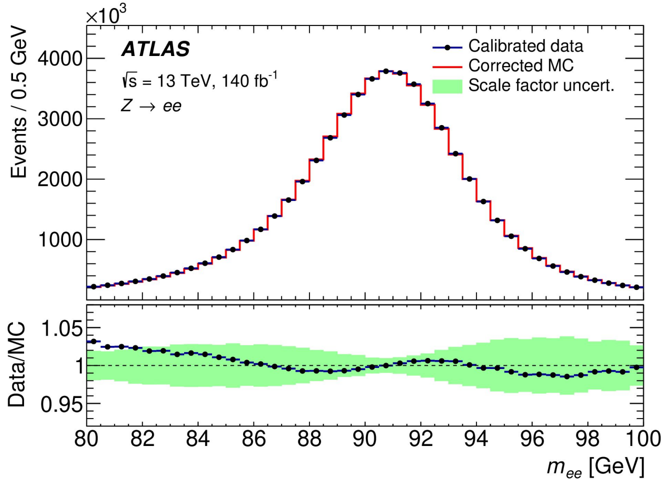

- Electron calibration relies on multiple steps to correct energy response of electrons
  - Corrections to match data and MC energy response/resolution
  - Correction to recover missing information in raw energy

- Data and MC agreement for the Z → ee invariant mass after energy scale correction is applied

Electrons

Eur. Phys. J. C 79 (2019) 639
JINST 19 (2024) P02009

Identification

- Likelihood discriminants constructed from shower shape and track-based variables that can discriminate prompt electrons from different backgrounds:
  - **Fake electrons** including energy deposits from hadronic jets or converted photons
  - **Non-prompt electrons** produced in heavy flavour decays

Slides by Otilia Ducu

- Three ID working points are defined with different efficiencies and fake rates
  - Tight WP provides the best background rejection at the expense of smaller efficiency
- Optimised in bins of η and E_T using $Z \rightarrow ee$ data and MC simulation

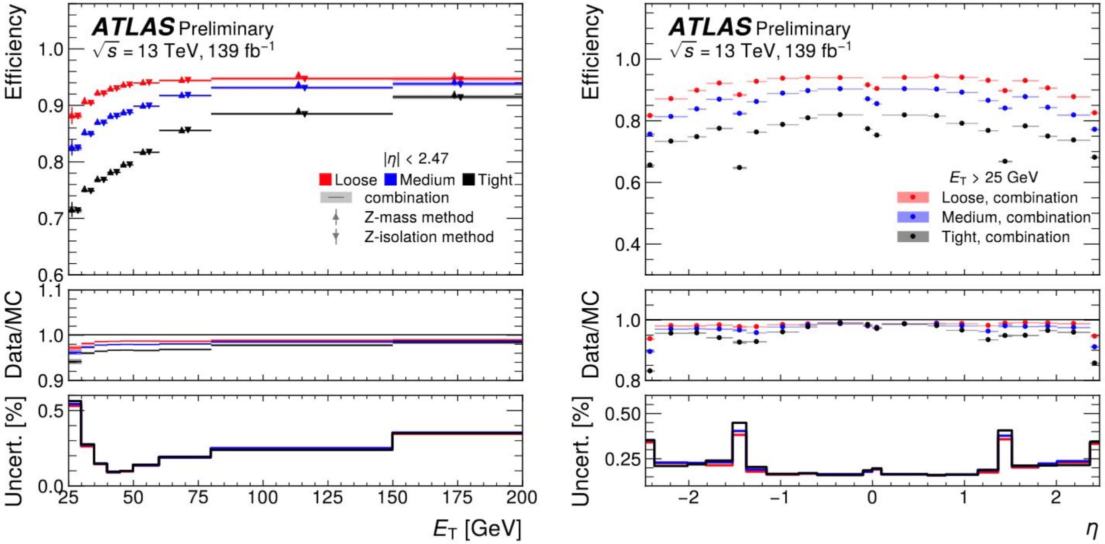

Lepton isolation

[Isolation efficiency for muons]

- Leptons (electrons and muons) from prompt decays of W/Z bosons can be discriminated from leptons from hadronic sources by measuring the amount of hadronic activity in their vicinity (isolation)

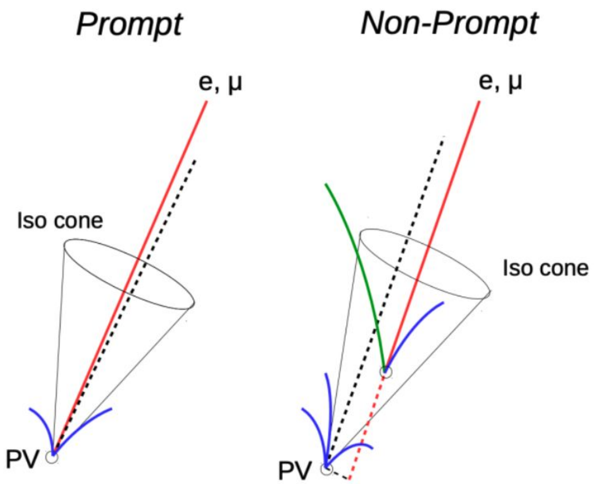

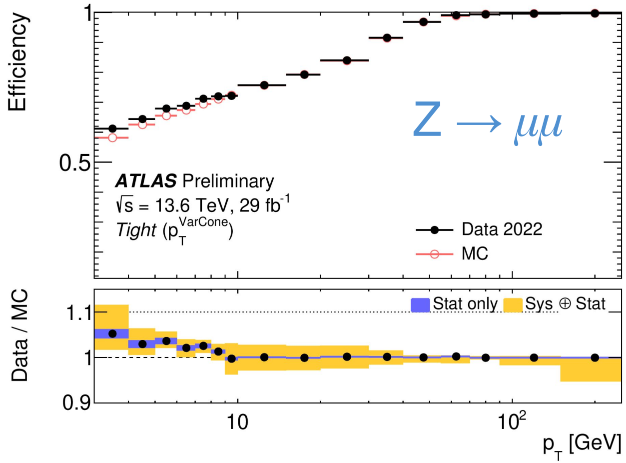

[Slides by Marco Sessa]

- **Track** isolation variables with variable cone sizes and **calorimeter** isolation variables are defined to reject background from different sources
- Several working points that compromise between highly-efficient identification of prompt leptons and good background rejection

Missing Transverse Momentum

CERN-EP-2024-023

$$\boldsymbol{p}_{\mathrm{T}}^{\mathrm{miss}} = -\Bigg(\underbrace{\sum_{\substack{\text{selected}\\ \text{electrons}}} \boldsymbol{p}_{\mathrm{T}}^{e} + \sum_{\substack{\text{accepted}\\ \text{photons}}} \boldsymbol{p}_{\mathrm{T}}^{\gamma} + \sum_{\substack{\text{accepted}\\ \tau-\text{leptons}}} \boldsymbol{p}_{\mathrm{T}}^{\tau} + \sum_{\substack{\text{selected}\\ \mu}} \boldsymbol{p}_{\mathrm{T}}^{\mu} + \sum_{\substack{\text{accepted}\\ \text{jets}}} \boldsymbol{p}_{\mathrm{T}}^{\text{jet}}}_{\text{hard term}} + \underbrace{\sum_{\substack{\text{unused}\\ \text{tracks}}} \boldsymbol{p}_{\mathrm{T}}^{\text{track}}}_{\text{soft term}} \Bigg)$$

- p_T^{miss}: Experimental proxy for the transverse momentum carried by undetected particles in the collision
  - Neutrinos from W $\rightarrow \ell\nu$ decays pass through without interacting with detector
  - Transverse momentum inferred using momentum conservation in the transverse plane after negative vector sum of p_T of all hard objects in event (electrons, muons, jets, etc.)
  - Remaining/unused tracks and jets with small p_T become the "track soft term"
- $Z \rightarrow \ell\ell$ + (0, …, N_{jet}) events used to study fake p_T^{miss} performance
- W $\rightarrow \mu\nu$ events (among others) are used to study real p_T^{miss} performance
- Tighter working points improve p_T^{miss} resolution at higher pile-up by removing more pile-up from jet term

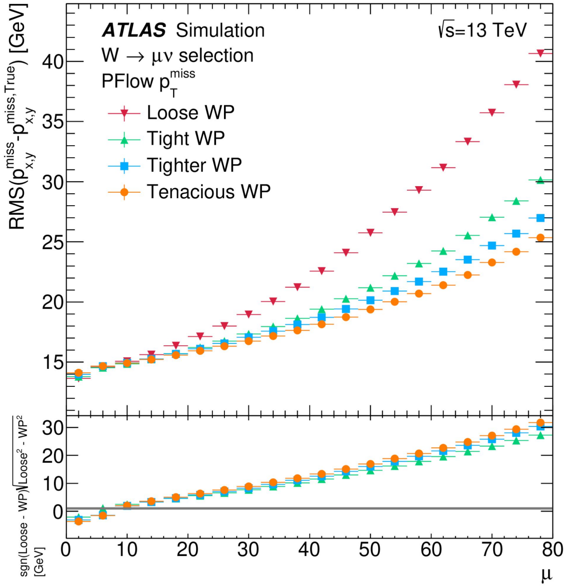

W/Z cross section measurement at √s = 13.6 TeV

- Measurement of the inclusive W/Z production cross sections and their ratios
  - Leptonic final states used for reconstruction and signal identification
  - ttbar/W ratio also calculated using recently published ttbar results ([PLB 848 (2024) 138376](PLB 848 (2024) 138376))
- Test theoretical predictions at the new centre-of-mass energy of 13.6 TeV
- Large cross sections and easily identifiable leptonic decays of the W and Z bosons provide a clean experimental signature
  - Important for early validation of detector performance and software

EUROPEAN ORGANISATION FOR NUCLEAR RESEARCH (CERN)

ATLAS EXPERIMENT

arXiv:2403.12902

Submitted to: Phys. Lett. B.

CERN-EP-2024-069
25th March 2024

Measurement of vector boson production cross sections and their ratios using pp collisions at $\sqrt{s}$ = 13.6 TeV with the ATLAS detector

The ATLAS Collaboration

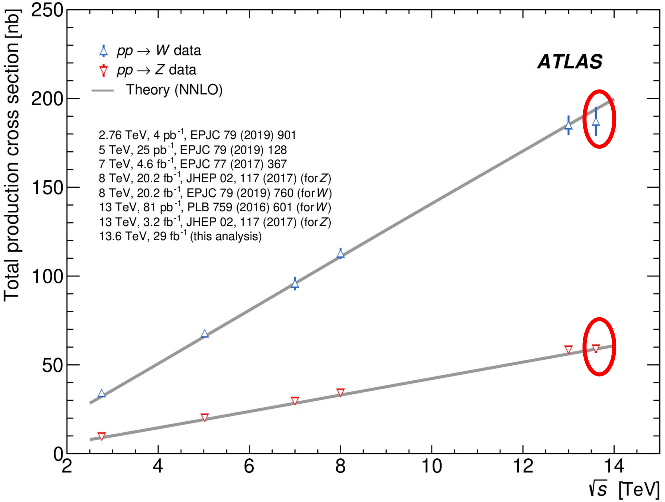

Data

[ATLAS Luminosity Results for Run-3](#)

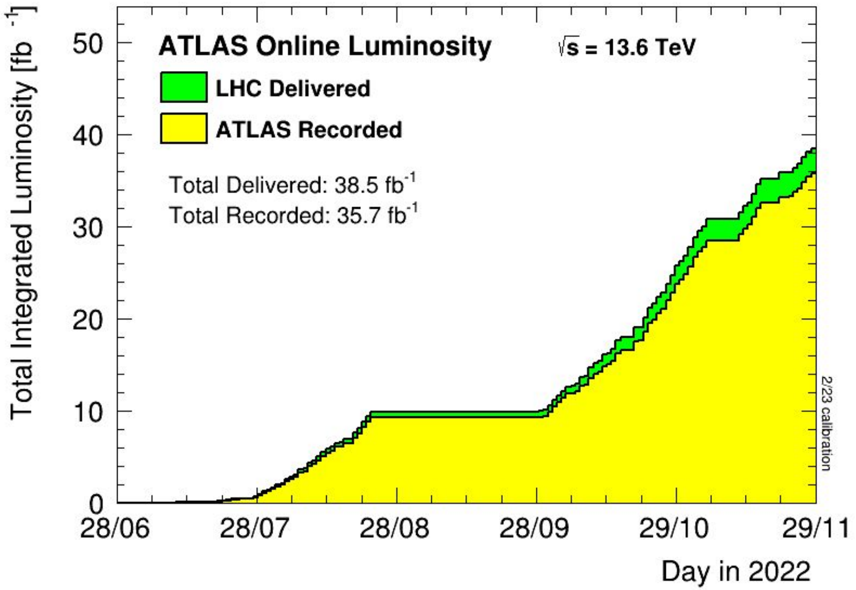

- Measurement performed using 2022 data from the beginning of Run-3
  - 29 fb^{-1} after data quality requirements
- Selected using a combination of single electron and muon triggers
  - Lowest threshold triggers with tighter isolation and identification criteria maximise number of events
  - Higher threshold triggers with relaxed or no isolation requirements to recover efficiency at high lepton p_T
  - Pre-scaled support triggers with no isolation requirements are used to select events for background estimation

Event selection

Electrons: p_T > 27 GeV, TightLH identification, tight isolation
Muons: p_T > 27 GeV, medium quality, tight isolation
Z-boson selection: 2 opposite sign, same flavour leptons, $66 < m_{ll} < 116$ GeV
W-boson selection: only 1 lepton, E_T^{miss} > 25 GeV, m_T^W > 50 GeV

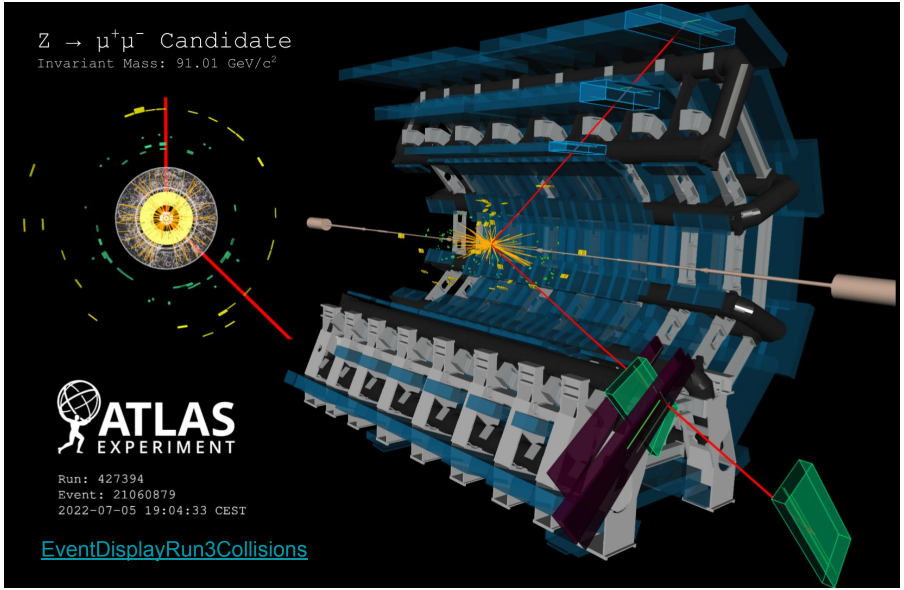

$$m_T^W = \sqrt{2 p_T^{\nu} p_T^{\ell} (1 - \cos \Delta\phi^{\nu})}$$

estimated using E_T^{miss}

lepton p_T

$\Delta\phi$ between lepton and E_T^{miss}

Background modelling

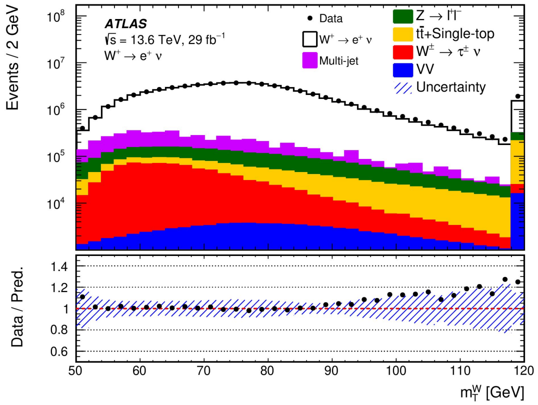

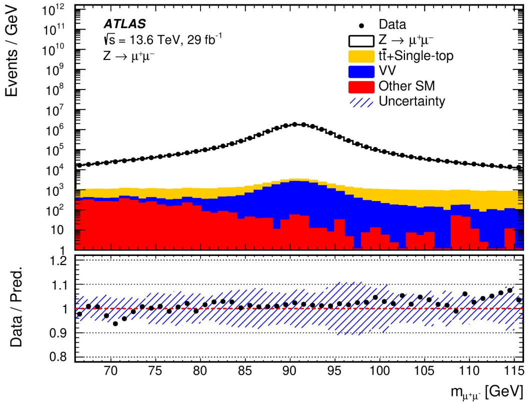

- EW + top background: estimated using **simulation**
  - Diboson (VV): one of the bosons decays hadronically or invisibly
  - Ttbar + single-top: (semi-)leptonic decay mode with one e/μ
  - Z → ee/$\mu\mu$: where one e/μ is not identified and E_T^{miss} from mis-measured hadronic energy
  - W →$\tau\nu$: where τ decays into e/μ
- Multi-jet: estimated using **data-driven method**
  - Fake electrons and energy mis-measurement from diverse QCD processes
  - Semi-leptonic heavy-quark decays resulting in real but non-prompt electron or muon

Data-driven background estimation

- Major source of background in W channels is **multijet**
- Diverse background composition including fake leptons and energy mis-measurement
  - Cannot be modelled accurately using simulation
- Multijets concentrated at lower values of E_T^{miss} and m_T^W than signal
- Event categories corresponding to different regions in phase space and **isolation**
  - Events selected in control regions using support triggers with no isolation requirements and anti-isolated leptons for higher multijet yield
  - **Scan track isolation** to reduce isolation bias

Fit region (FR)	Signal region (SR)
• Lepton p_T > 27 GeV • E_T^{miss} < 25 GeV • m_T^W < 50 GeV • Pass isolation	• Lepton p_T > 27 GeV • E_T^{miss} > 25 GeV • m_T^W > 50 GeV • Pass isolation
Control region 1 (CR1) • Lepton p_T > 27 GeV • E_T^{miss} < 25 GeV • m_T^W < 50 GeV • Fail isolation	**Control region 2 (CR2)** • Lepton p_T > 27 GeV • E_T^{miss} > 25 GeV • m_T^W > 50 GeV • Fail isolation

Lepton isolation CRs

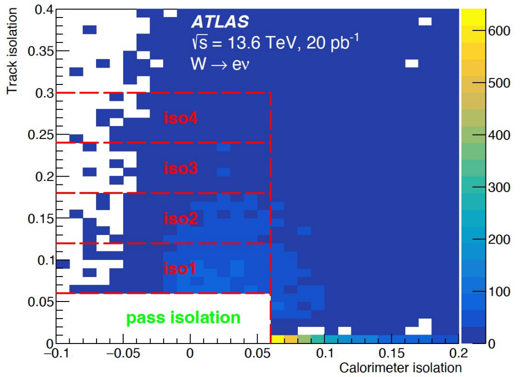

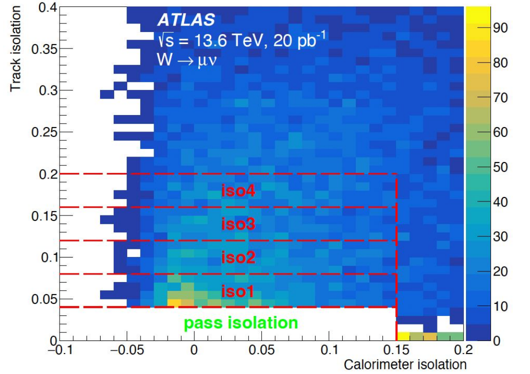

Data-driven background estimation

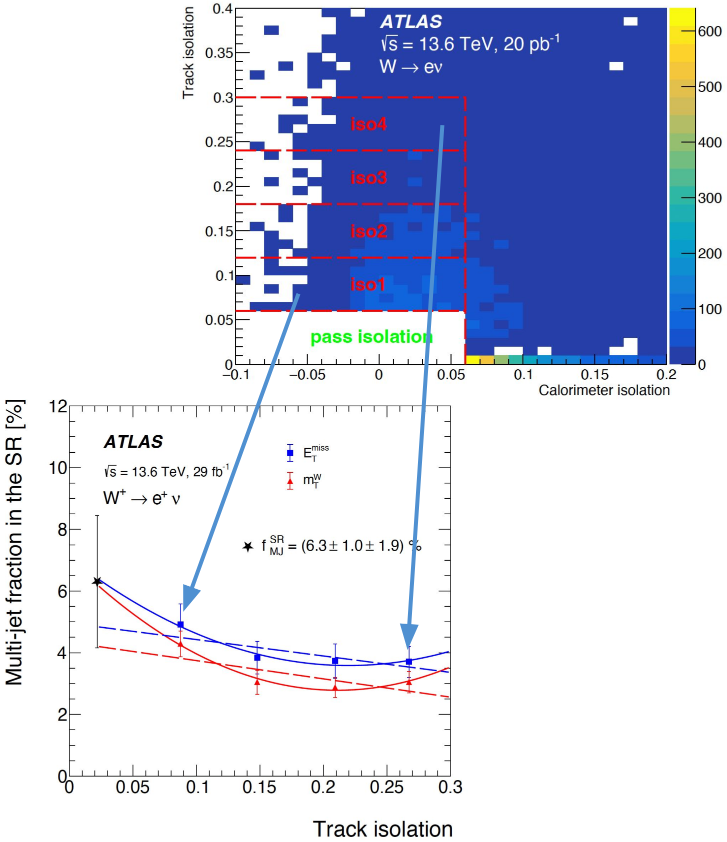

- Multijet templates derived from control regions requiring leptons to **fail isolation**
  - Support triggers used to select events in control regions
  - EW+top contamination subtracted from data, estimated using MC
- Several multijet templates created from several **isolation slices** in control regions
- Multijet normalisation from profile-likelihood fits in a fitting region
  - Extract normalisation using multijet templates from 4 isolation slices and 2 discriminating variables (E_T^{miss} and m_T^W) in each channel
- Perform extrapolation in track isolation in order to reduce isolation bias on final multijet yield
  - Central value obtained from quadratic fit result with difference between linear and quadratic fit results as additional uncertainty

Cross section measurement

- Fiducial cross sections are extracted with **binned profile likelihood fits** using 8 channels:
  - 2 Z-boson channels (ee and μμ), 4 W-boson channels ($e^+\nu$, $e^-\nu$, $\mu^+\nu$ and $\mu^-\nu$) and 2 ttbar channels (eμ with 1 b-jet and eμ with 2 b-jets)

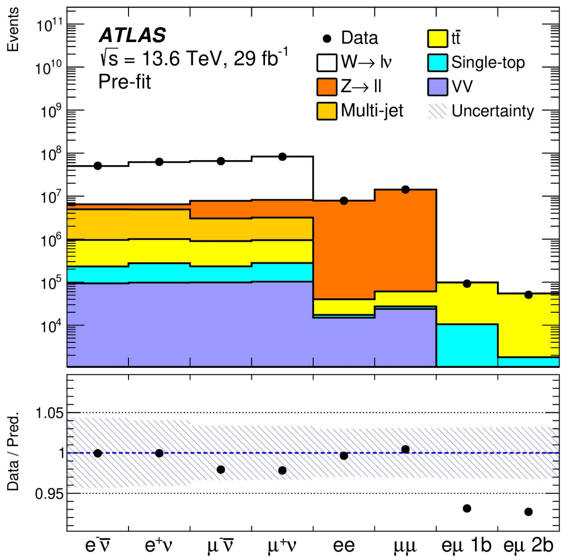

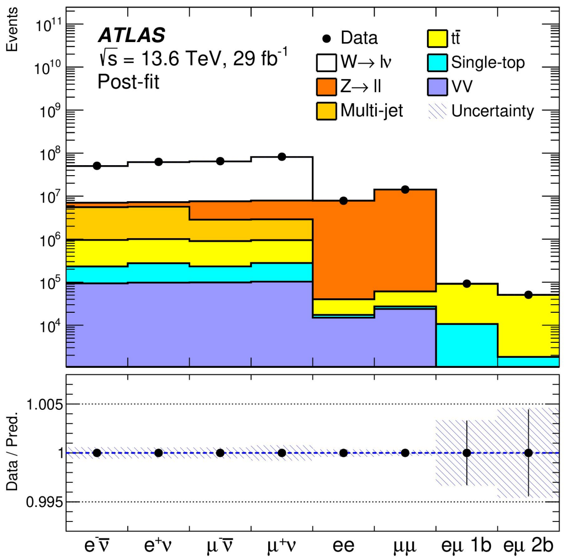

Results: fiducial cross sections

- Fiducial cross sections compared to theoretical predictions calculated with different PDF sets
  - Theoretical predictions are calculated to NNLO + NNLL QCD accuracy and NLO EW accuracy
  - Good agreement between results and SM predictions

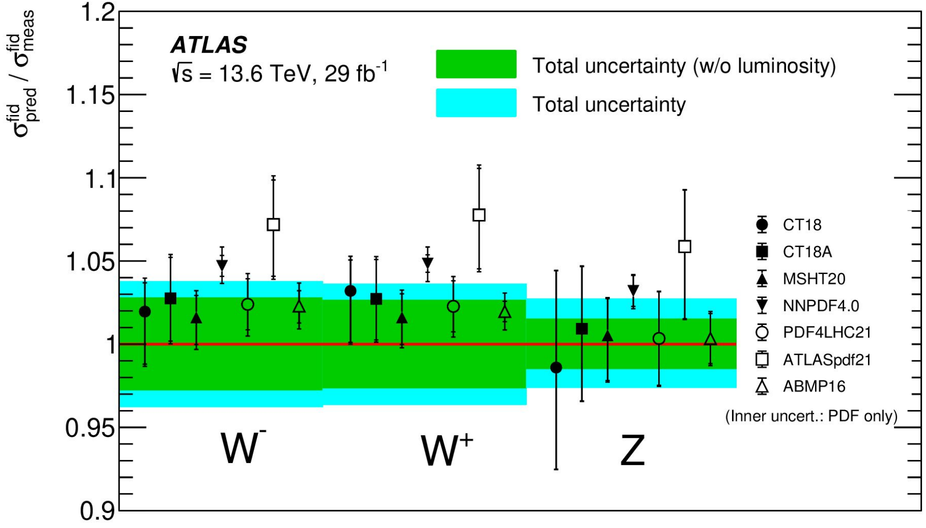

Channel	$\sigma^{fid} \pm \delta\sigma_{stat.+syst.}$ [pb]
$Z \to e^+e^-$	740 ± 22
$Z \to \mu^+\mu^-$	747 ± 23
$\boxed{Z \to \ell^+\ell^-}$	$\boxed{744 \pm 20}$
$W^- \to e^-\bar{\nu}$	3380 ± 170
$W^- \to \mu^-\bar{\nu}$	3310 ± 130
$\boxed{W^- \to \ell^-\bar{\nu}}$	$\boxed{3310 \pm 120}$
$W^+ \to e^+\nu$	4350 ± 200
$W^+ \to \mu^+\nu$	4240 ± 160
$\boxed{W^+ \to \ell^+\nu}$	$\boxed{4250 \pm 150}$
$W^\pm \to \ell^\pm\nu$	7560 ± 270

Results: fiducial cross sections

- Fiducial cross sections compared to theoretical predictions calculated with different PDF sets
  - Theoretical predictions are calculated to NNLO + NNLL QCD accuracy and NLO EW accuracy
  - Good agreement between results and SM predictions

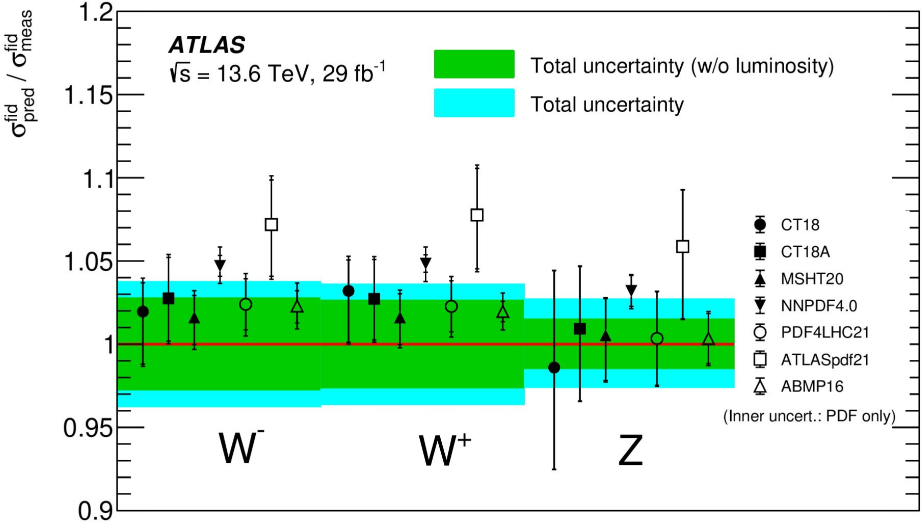

- Dominant sources of uncertainties:
  - $W^{\pm}$: luminosity, jet and multi-jet background
  - Z: luminosity, lepton efficiency

Category	$\sigma(W^- \to \ell^-\bar{\nu})$	$\sigma(W^+ \to \ell^+\nu)$	$\sigma(W^\pm \to \ell\nu)$	$\sigma(Z \to \ell\ell)$
Luminosity	2.5	2.4	2.4	2.2
Pile-up	0.5	0.7	0.6	0.8
MC statistics	< 0.2	0.2	< 0.2	< 0.2
Lepton trigger	1.0	0.9	0.9	0.2
Electron reconstruction	0.4	0.5	0.4	0.9
Muon reconstruction	0.6	0.6	0.6	1.4
Multi-jet	1.2	1.2	1.2	–
Other background modelling	0.4	0.4	0.4	< 0.2
Jet energy scale	1.3	1.3	1.3	–
Jet energy resolution	< 0.2	0.2	< 0.2	–
NNJVT	1.4	1.3	1.3	–
E_T^{miss} track soft term	< 0.2	0.3	0.3	–
PDF	0.5	0.5	0.3	< 0.2
QCD scale (ME and PS)	0.8	0.7	0.6	0.3
Flavour tagging	–	–	–	–
$t\bar{t}$ modelling	–	–	–	–
Total systematic impact [%]	3.7	3.5	3.5	2.7
Statistical impact [%]	0.01	0.01	0.01	0.02

Results: fiducial cross sections

- Fiducial cross sections compared to theoretical predictions calculated with different PDF sets
  - Theoretical predictions are calculated to NNLO + NNLL QCD accuracy and NLO EW accuracy
  - Good agreement between results and SM predictions

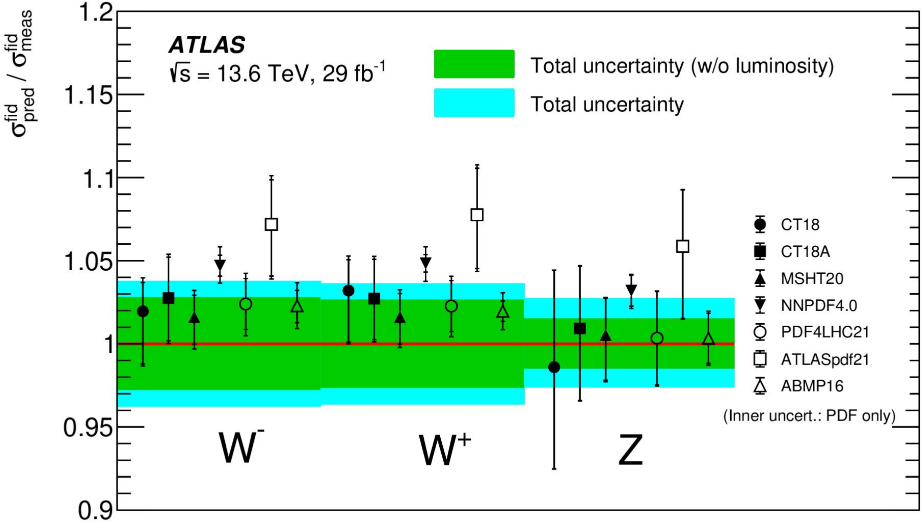

- Dominant sources of uncertainties:
  - $W^{\pm}$: luminosity, jet and multi-jet background
  - Z: luminosity, lepton efficiency

Category	$\sigma(W^- \to \ell^- \bar{\nu})$	$\sigma(W^+ \to \ell^+ \nu)$	$\sigma(W^{\pm} \to \ell \nu)$	$\sigma(Z \to \ell\ell)$
Luminosity	2.5	2.4	2.4	2.2
Pile-up	0.5	0.7	0.6	0.8
MC statistics	< 0.2	0.2	< 0.2	< 0.2
Lepton trigger	1.0	0.9	0.9	0.2
Electron reconstruction	0.4	0.5	0.4	0.9
Muon reconstruction	0.6	0.6	0.6	1.4
Multi-jet	1.2	1.2	1.2	–
Other background modelling	0.4	0.4	0.4	< 0.2
Jet energy scale	1.3	1.3	1.3	–
Jet energy resolution	< 0.2	0.2	< 0.2	–
NNJVT	1.4	1.3	1.3	–
E_T^{miss} track soft term	< 0.2	0.3	0.3	–
PDF	0.5	0.5	0.3	< 0.2
QCD scale (ME and PS)	0.8	0.7	0.6	0.3
Flavour tagging	–	–	–	–
$t\bar{t}$ modelling	–	–	–	–
Total systematic impact [%]	3.7	3.5	3.5	2.7
Statistical impact [%]	0.01	0.01	0.01	0.02

Results: cross-section ratios

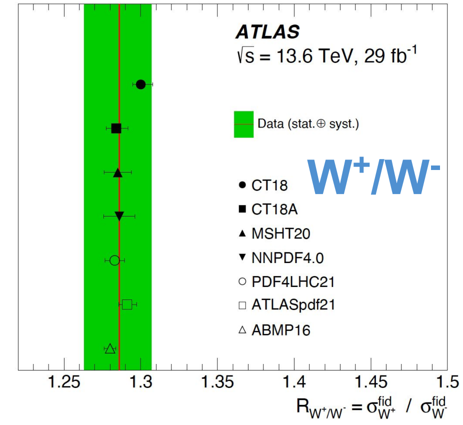

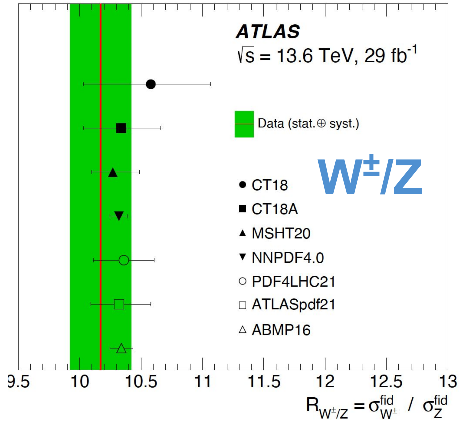

- Cross-section ratios benefit from cancellations of some of the experimental uncertainties
- Good agreement between W/Z results and SM predictions
  - ttbar/W± ratio shows slight deviations from the theoretical predictions

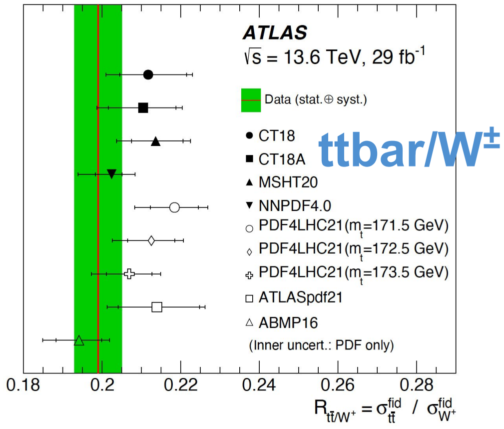

Ratio	$R \pm \delta R_{\text{stat.+syst.}}$
W^+/W^-	1.286 ± 0.022
$W^\pm/Z$	10.17 ± 0.25
$t\bar{t}/W^-$	0.256 ± 0.008
$t\bar{t}/W^+$	0.199 ± 0.006
$t\bar{t}/W^\pm$	0.112 ± 0.003

Results: cross-section ratios

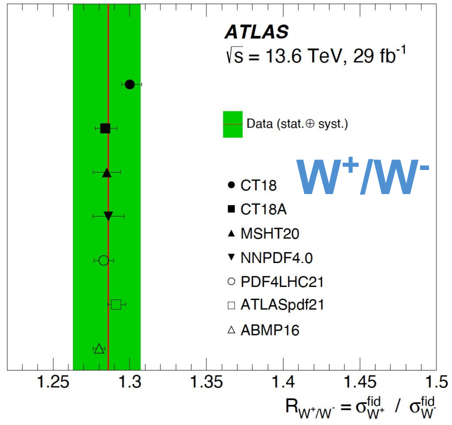

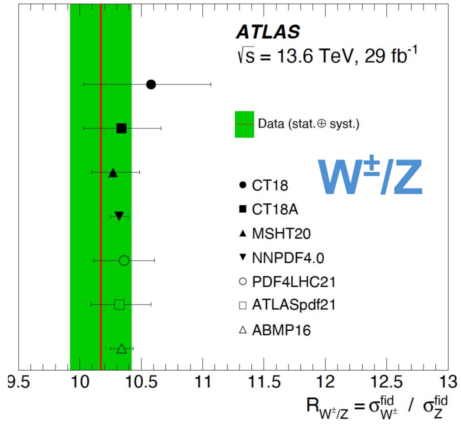

- Cross-section ratios benefit from cancellations of some of the experimental uncertainties
- Good agreement between W/Z results and SM predictions
  - ttbar/W$^\pm$ ratio shows slight deviations from the theoretical predictions

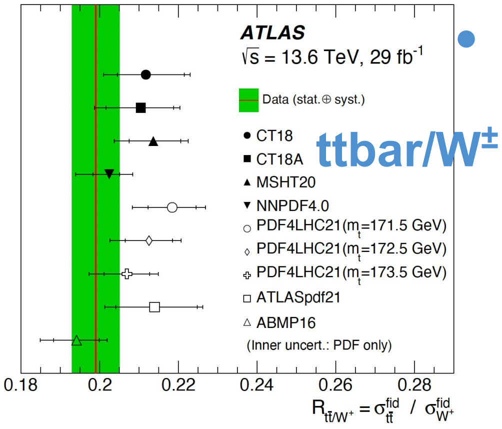

- Dominant sources of uncertainties:
  - W$^+$/W$^-$: multi-jet background
  - W$^\pm$/Z: jet related uncertainty
  - ttbar/W$^\pm$: ttbar modelling, jet and multi-jet background

Category	R_{W^+/W^-}	$R_{W^\pm/Z}$	$R_{t\bar{t}/W^\pm}$
Luminosity	< 0.2	0.3	< 0.2
Pile-up	< 0.2	< 0.2	< 0.2
MC statistics	< 0.2	< 0.2	< 0.2
Lepton trigger	< 0.2	0.7	0.8
Electron reconstruction	< 0.2	0.5	0.4
Muon reconstruction	0.2	0.8	0.6
Multi-jet	1.6	1.1	1.0
Other background modelling	< 0.2	0.3	0.9
Jet energy scale	< 0.2	1.3	1.3
Jet energy resolution	< 0.2	< 0.2	< 0.2
NNJVT	< 0.2	1.3	< 0.2
E_T^{miss} track soft term	< 0.2	0.3	0.3
PDF	0.5	0.2	0.4
QCD scale (ME and PS)	< 0.2	0.7	0.7
Flavour tagging	–	–	< 0.2
$t\bar{t}$ modelling	–	–	1.1
Total systematic impact [%]	1.7	2.4	2.5
Statistical impact [%]	0.01	0.02	0.32

Results: cross-section ratios

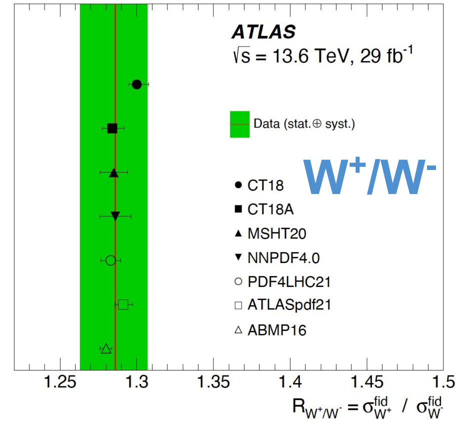

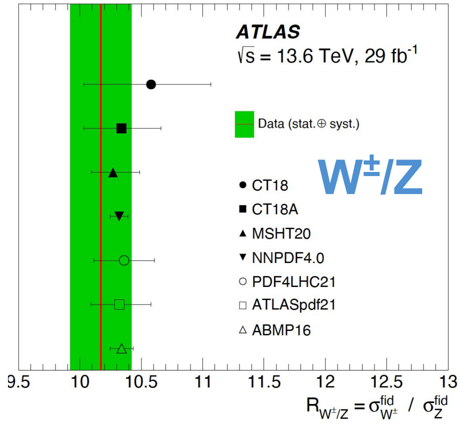

- Cross-section ratios benefit from cancellations of some of the experimental uncertainties
- Good agreement between W/Z results and SM predictions
  - ttbar/W$^\pm$ ratio shows slight deviations from the theoretical predictions

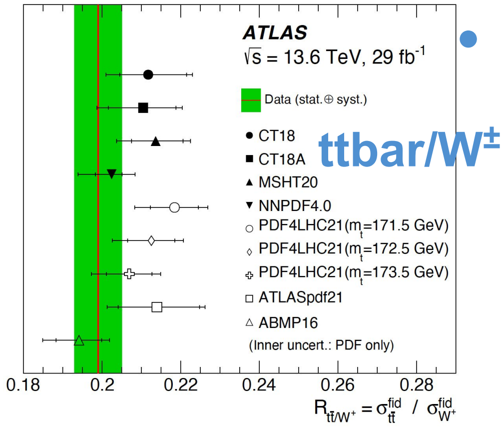

- Dominant sources of uncertainties:
  - W$^+$/W$^-$: multi-jet background
  - W$^\pm$/Z: jet related uncertainty
  - ttbar/W$^\pm$: ttbar modelling, jet and multi-jet background

Category	R_{W^+/W^-}	$R_{W^\pm/Z}$	$R_{t\bar{t}/W^\pm}$
Luminosity	< 0.2	0.3	< 0.2
Pile-up	< 0.2	< 0.2	< 0.2
MC statistics	< 0.2	< 0.2	< 0.2
Lepton trigger	< 0.2	0.7	0.8
Electron reconstruction	< 0.2	0.5	0.4
Muon reconstruction	0.2	0.8	0.6
Multi-jet	1.6	1.1	1.0
Other background modelling	< 0.2	0.3	0.9
Jet energy scale	< 0.2	1.3	1.3
Jet energy resolution	< 0.2	< 0.2	< 0.2
NNJVT	< 0.2	1.3	< 0.2
E_T^{miss} track soft term	< 0.2	0.3	0.3
PDF	0.5	0.2	0.4
QCD scale (ME and PS)	< 0.2	0.7	0.7
Flavour tagging	–	–	< 0.2
$t\bar{t}$ modelling	–	–	1.1
Total systematic impact [%]	1.7	2.4	2.5
Statistical impact [%]	0.01	0.02	0.32

Results: cross-section ratios

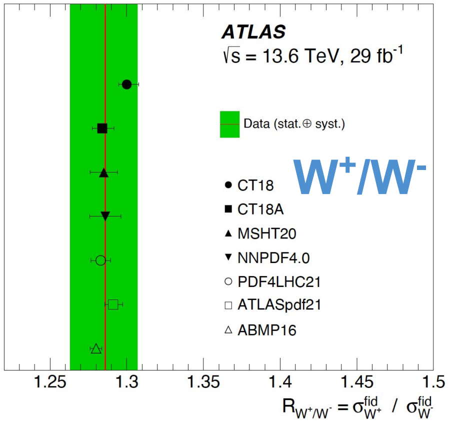

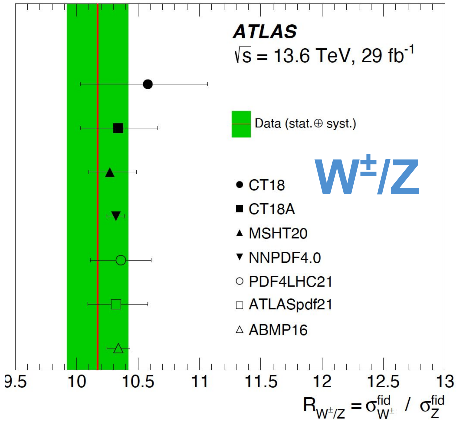

- Cross-section ratios benefit from cancellations of some of the experimental uncertainties
- Good agreement between W/Z results and SM predictions
  - ttbar/W$^\pm$ ratio shows slight deviations from the theoretical predictions

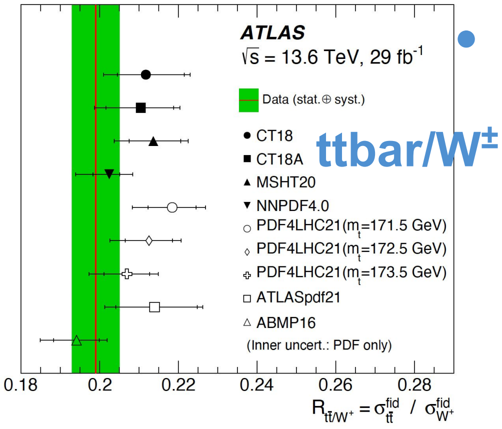

- Dominant sources of uncertainties:
  - W^+/W^-: multi-jet background
  - $W^\pm/Z$: jet related uncertainty
  - ttbar/W$^\pm$: ttbar modelling, jet and multi-jet background

Category	R_{W^+/W^-}	$R_{W^\pm/Z}$	$R_{t\bar{t}/W^\pm}$
Luminosity	< 0.2	0.3	< 0.2
Pile-up	< 0.2	< 0.2	< 0.2
MC statistics	< 0.2	< 0.2	< 0.2
Lepton trigger	< 0.2	0.7	0.8
Electron reconstruction	< 0.2	0.5	0.4
Muon reconstruction	0.2	0.8	0.6
Multi-jet	1.6	1.1	1.0
Other background modelling	< 0.2	0.3	0.9
Jet energy scale	< 0.2	1.3	1.3
Jet energy resolution	< 0.2	< 0.2	< 0.2
NNJVT	< 0.2	1.3	< 0.2
E_T^{miss} track soft term	< 0.2	0.3	0.3
PDF	0.5	0.2	0.4
QCD scale (ME and PS)	< 0.2	0.7	0.7
Flavour tagging	–	–	< 0.2
$t\bar{t}$ modelling	–	–	1.1
Total systematic impact [%]	1.7	2.4	2.5
Statistical impact [%]	0.01	0.02	0.32

Summary

- Measuring the W and Z boson cross sections provides a benchmark for our understanding of QCD and EW processes
- Large cross sections and clean experimental signatures from leptonic decays allow percent-level experimental precision (sub-percent level for ratios)
  - Sensitive to PDFs
  - Essential for detector performance
- Measurement of W and Z cross sections and their ratios at $\sqrt{s}$ = 13.6 TeV
  - ttbar/W ratio also measured for the first time in ATLAS
  - Good agreement between results and predictions calculated with different PDF sets